The Journal of Experimental Biology 202, 429–440 (1999)
Printed in Great Britain © The Company of Biologists Limited 1999
JEB1753

P-TYPE Ca^{2+} CURRENT IN CRAYFISH PEPTIDERGIC NEURONES

JESÚS GARCÍA-COLUNGA[1], RENÉ VALDIOSERA[2] AND UBALDO GARCÍA[2,*]

[1]*Center of Neurobiology, National University of Mexico, Campus Juriquilla, Querétaro, 76001 México* and
[2]*Department of Physiology, Biophysics and Neuroscience, CINVESTAV, 07000 México*

*Author for correspondence (e-mail: ugarcia@fisio.cinvestav.mx)

Accepted 18 November 1998; published on WWW 21 January 1999

Summary

Inward Ca^{2+} current through voltage-gated Ca^{2+} channels was recorded from freshly dissociated crayfish X-organ (XO) neurones using the whole-cell voltage-clamp technique. Changing the holding potential from –50 to –90 mV had little effect on the characteristics of the current–voltage relationship: neither the time course nor the amplitude of the Ca^{2+} current was affected. Inactivation of the Ca^{2+} current was observed over a small voltage range, between –35 and –10 mV, with half-inactivation at –20 mV. The activation of the Ca^{2+} current was modelled using Hodgkin–Huxley kinetics. The time constant of activation, τ_m, was 568±66 μs at –20 mV and decreased gradually to 171±23 μs at 40 mV (means ± S.E.M., N=5). The steady-state activation, m_∞, was fitted with a Boltzmann function, with a half-activation voltage of –7.45 mV and an apparent threshold at –40 mV. The instantaneous current–voltage relationship was adjusted using the Goldman–Hodgkin–Katz constant-field equation, giving a permeation of 4.95×10^{-5} cm s^{-1}. The inactivation of the Ca^{2+} current in XO neurones was dependent on previous entry of Ca^{2+}. Using a double-pulse protocol, the inactivation was fitted to a U-shaped curve with a maximal inactivation of 35 % at 30 mV. The time course of the recovery from inactivation was fitted with an exponential function. The time constants were 17±2.6 ms for a prepulse of 10 ms and 31±3.2 ms for a prepulse of 20 ms. The permeability sequence of the Ca^{2+} channels was as follows: $Ba^{2+}>Sr^{2+}\approx Ca^{2+}\gg Mg^{2+}$. Other divalent cations blocked the Ca^{2+} current, and their effects were voltage-dependent; the potency of blockage was $Cd^{2+}\approx Zn^{2+}\gg Co^{2+}\approx Ni^{2+}$. The peptide ω-agatoxin-IVA, a selective toxin for P-type Ca^{2+} channels, blocked 85 % of the Ca^{2+} current in XO neurones at 200 nmol l^{-1}, but the current was insensitive to dihydropyridines, phenylalkylamines, ω-conotoxin-GVIA and ω-conotoxin-MVIIC, which are blockers of L-, N- and Q-type Ca^{2+} channels, respectively. From the voltage- and Ca^{2+}-dependent kinetics, the higher permeability to Ba^{2+} than to Ca^{2+} and the higher sensitivity of the current to Cd^{2+} than to Ni^{2+}, we conclude that the Ca^{2+} current in XO neurones is generated by high-voltage-activated (HVA) channels. Furthermore, its blockage by ω-agatoxin-IVA suggests that it is mainly generated through P-type Ca^{2+} channels.

Key words: P-type Ca^{2+} current, ω-agatoxin-IVA, crayfish, peptidergic neurone, *Procambarus clarkii*.

Introduction

Entry of Ca^{2+} through voltage-dependent Ca^{2+} channels plays an important role in excitable cells and is related to their electrical activity. The opening of Ca^{2+} channels transiently increases the intracellular free Ca^{2+} concentration, which acts as messenger and may control ion channel gating, enzyme activation, gene expression, transmitter release, neurosecretion and other cell functions (for reviews, see Llinás et al., 1992; Miller, 1992; Tsien and Tsien, 1990).

Several classes of voltage-dependent Ca^{2+} channel have been identified in vertebrates on the basis of electrophysiological and pharmacological criteria and by molecular cloning (Sather et al., 1993; Snutch and Reiner, 1992). They are classified as low-voltage-activated (LVA) and high-voltage-activated (HVA) Ca^{2+} channels (Carbone and Lux, 1984; Fox et al., 1987; Swandulla et al., 1991; Tsien et al., 1988). LVA or T-type Ca^{2+} channels are sensitive to Ni^{2+}, amiloride, ethosuximide and octanol and are insensitive to 1,4-dihydropyridines (DHPs), ω-conotoxin-GVIA and ω-agatoxin-IVA (Coulter et al., 1989; Herrington and Lingle, 1992; Mori, 1994; Tang et al., 1988). HVA Ca^{2+} channels have been subdivided into five types: (a) L-type channels sensitive to DHPs (Fox et al., 1987; Hess et al., 1984); (b) N-type channels insensitive to DHPs and irreversibly blocked by ω-conotoxin-GVIA (Aosaki and Kasai, 1989; Plummer et al., 1989); (c) P-type channels insensitive to DHPs and to ω-conotoxin GVIA but selectively blocked by nanomolar concentrations of ω-agatoxin-IVA (<30 nmol l^{-1}) (Llinás et al., 1989; Mintz et al., 1992) and by funnel-web spider toxin (Wang and Lemos, 1994); (d) Q-type channels blocked by ω-agatoxin-TK and by higher concentrations of ω-agatoxin IVA (>100 nmol l^{-1}) and which differ from P-type channels in their sensitivity to ω-conotoxin-MVIIC (<150 nmol l^{-1}) (Hillyard et

al., 1992; Wang et al., 1997); and finally (e) R-type channels insensitive to organic compounds and blocked by Ni^{2+} (Zhang et al., 1993).

In contrast, few studies have been carried out on Ca^{2+} channels in invertebrate neurones. Both LVA and HVA Ca^{2+} current types have been identified in leech (Angstadt and Calabrese, 1991), snail (Haydon and Man-Son-Hing, 1988), *Aplysia californica* (Fossier et al., 1994), squid (Llinás et al., 1989) and crustacean neurones (Meyers et al., 1992; Onetti et al., 1990; Richmond et al., 1995, 1996). Recently, a P-type Ca^{2+} channel has been described in crayfish motoneurones (Hong and Lnenicka, 1997) that is less sensitive to ω-agatoxin-IVA (600 nmol l^{-1}) than that in vertebrate neurones (Randall and Tsien, 1995).

Spontaneous neuronal firing in the X-organ sinus gland system is related to hormonal release (Stuenkel, 1985). Action potentials are Ca^{2+}-dependent (Iwasaki and Satow, 1971) and the intracellular free [Ca^{2+}] modulates K^+ channels (Martínez et al., 1991) and the negative slope conductance (Onetti et al., 1990). In the present study, we characterize the biophysical and pharmacological properties of the Ca^{2+} current in freshly dissociated XO neurones of the crayfish *Procambarus clarkii* and demonstrate that it corresponds to an HVA P-type Ca^{2+} current.

Materials and methods

Dissection

Procambarus clarkii (Girard) were collected from Río Conchos, Chihuahua, México, and acclimated to laboratory conditions for 2 weeks under a 12 h:12 h L:D photoperiod. Eyestalks were excised and placed in chilled saline solution containing (in mmol l^{-1}): 205 NaCl, 5.4 KCl, 2.6 $MgCl_2$, 13.5 $CaCl_2$ and 10 Hepes, adjusted to pH 7.4 with NaOH. The exoskeleton, muscles and connective tissue were carefully removed under a dissecting microscope, and the neuronal somata were exposed. Isolated XOs were incubated with 200 μg ml^{-1} collagenase-dispase (Boehringer Mannheim) for 1 h in modified Leibovitz L-15 culture medium containing (in mmol l^{-1}): 205 NaCl, 5.4 KCl, 13.5 $CaCl_2$, 2.5 $MgCl_2$, 10 Hepes, 5.5 glucose, 2 L-glutamine, and gentamycin (16 μg ml^{-1}, Schering Plough), streptomycin (5 μg ml^{-1}, Sigma) and penicillin (5 units ml^{-1}, Sigma). The enzyme was washed out, and the XO neurones were dissociated by gentle suction through fire-polished micropipettes (García et al., 1990). Isolated neurones were plated individually onto a 200 μl recording chamber, precoated with Concanavalin A (Type III, Sigma). Cells were maintained at room temperature (22–24 °C) in modified Leibovitz L-15 medium.

Electrophysiology

Voltage-clamp experiments in the whole-cell configuration were performed using freshly dissociated XO neurones (2–6 h after plating). Recordings were made using an Axopatch-200A amplifier (Axon Instruments). Pipettes were constructed from borosilicate capillaries (Sutter Instruments) using a horizontal puller (P-87 Flaming Brown, Sutter Instruments) and fire-polished with a microforge (Narishige MF-90), to a final resistance of 2.5–4 MΩ. Pipettes were filled with a solution containing (in mmol l^{-1}): 215 CsCl, 2.86 $CaCl_2$, 2 Mg-ATP, 5.25 EGTA, 10 Hepes, adjusted to pH 7.4 with CsOH. Ca^{2+} currents were filtered at 5 kHz and acquired using commercially available hardware and software (Axon Instruments). Transient capacitative and leak currents were subtracted using the P/4 protocol (Almers et al., 1983), series resistance was generally compensated >70 %. X-organ neurones were continuously superfused with a solution containing (in mmol l^{-1}): 195 *N*-methyl-D-glucamine chloride (NMG-Cl), 20 tetraethylammonium chloride (TEA-Cl), 13.5 $CaCl_2$ and 10 Hepes, adjusted to pH 7.4 with NMG^+. During permeability experiments, extracellular Ca^{2+} was substituted equimolarly by Ba^{2+}, Sr^{2+}, Mg^{2+}, Mn^{2+}, Cd^{2+}, Ni^{2+} or Co^{2+}; in blocking experiments, the divalent cations (Cd^{2+}, Ni^{2+}, Co^{2+} and Zn^{2+}) were added to the superfusing solution.

Pharmacology

Stock solutions of DHPs (nifedipine, nitrendipine and Bay K-8644) were dissolved in 95 % ethanol and stored in the dark at 4 °C. The DHPs tested (2–20 μmol l^{-1}) were protected from light during experiments. Peptide toxins (Alomone) were dissolved in dimethyl sulphoxide, and the concentrations tested were from 50 nmol l^{-1} to 5 μmol l^{-1}. Organic blockers were superfused with a low-[Ca^{2+}] solution containing (in mol l^{-1}): 207 NMG-Cl, 20 TEA-Cl, 5 $CaCl_2$ and 10 Hepes (pH 7.4).

Results

To characterize the properties of the Ca^{2+} current in freshly dissociated crayfish XO neurones, other membrane currents were minimized. The Na^+ current was eliminated by replacing external Na^+ with NMG^+; K^+ currents were blocked with TEA^+ (20 mmol l^{-1}) in the external solution and by substituting intracellular K^+ with Cs^+. Under these ionic conditions, membrane-depolarizing voltage pulses activated an inward current identified as a Ca^{2+} current.

Steady-state voltage-dependent activation of the Ca^{2+} current

Fig. 1A shows a set of recordings of inward Ca^{2+} currents in response to 10 mV depolarizing voltage steps from a holding potential of −70 mV. The threshold for the activation of the Ca^{2+} current was approximately –40 mV (Fig. 1A,B). Both the onset and decay of the Ca^{2+} current became faster as depolarization increased. The Ca^{2+} current reached its peak in approximately 2 ms at 20 mV. The current decayed in a time-dependent manner that reflected mainly inactivation of Ca^{2+} channels. The maximal Ca^{2+} current was evoked at potentials between 20 and 30 mV. The current–voltage (*I–V*) relationship (Fig. 1B) shows that depolarizations greater than 20 mV resulted in a progressive decrease in the amplitude of the Ca^{2+} current; the reversal potential was more positive than 80 mV.

To establish the presence of LVA Ca^{2+} currents in XO neurones, recordings were made from several cells at three

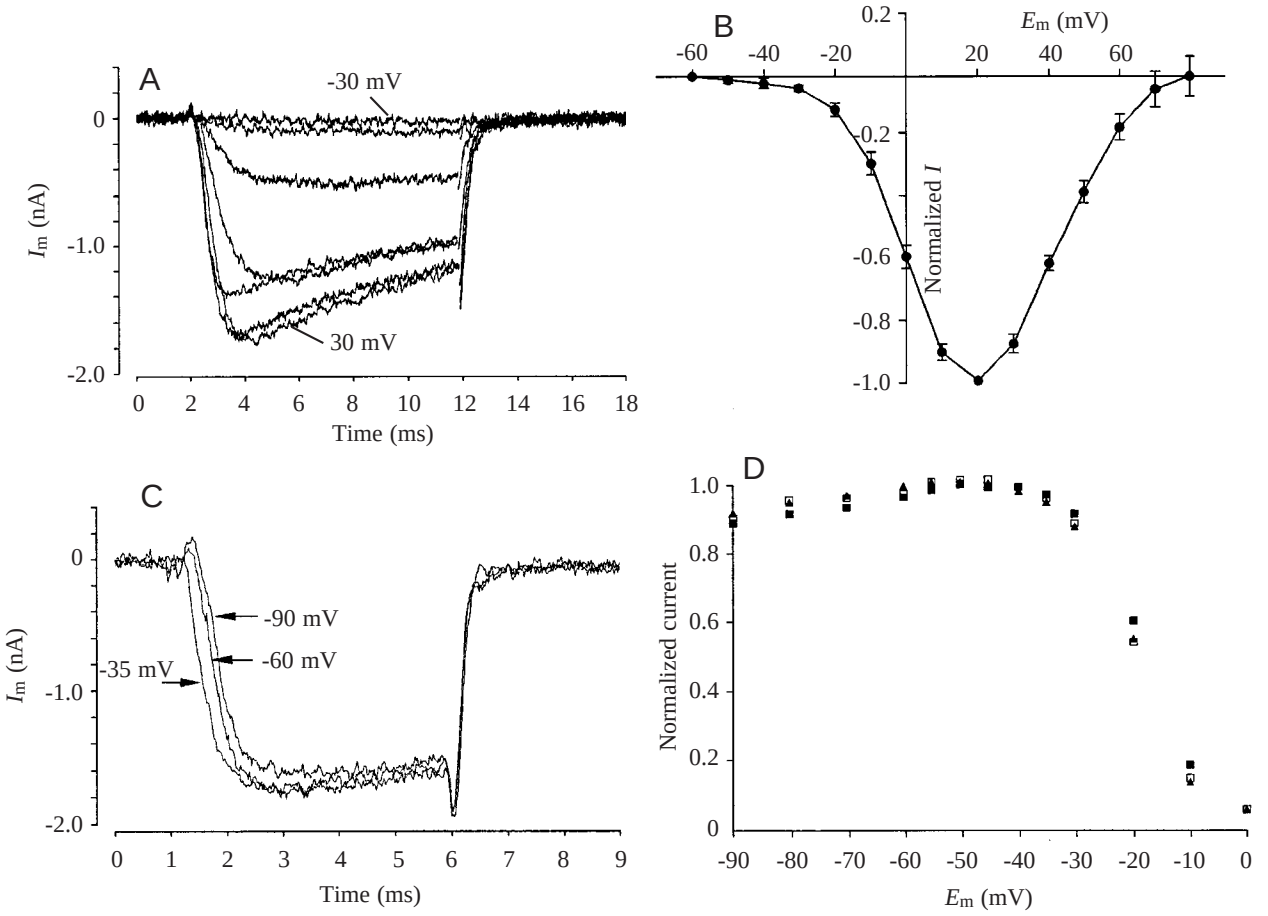

Fig. 1. Activation of the Ca^{2+} current in XO neurones. (A) Ca^{2+} current (I_m) traces obtained in response to 10 ms depolarizing command pulses and steps of 10 mV, from −30 to 30 mV. The holding potential was −70 mV. (B) Normalized Ca^{2+} current (I) amplitude as a function of membrane potential (E_m) (mean ± S.D. N=12). (C) Typical Ca^{2+} current traces recorded from the same neurone in response to a step to 30 mV from the three holding potentials indicated. (D) Normalized Ca^{2+} current amplitude from three neurones plotted against a holding potential ranging from −90 to 0 mV. The Ca^{2+} currents were evoked by depolarizing command pulses to 30 mV.

different holding potentials ranging from −90 to −40 mV. This manoeuvre is commonly used to remove the possible inactivation of such currents (Carbone and Lux, 1984; Kasai and Neher, 1992). The *I–V* relationships obtained from these experiments had the same threshold potential and current amplitudes, they also peaked at the same voltage, and the reversal potential was the same (data not shown). No differences were observed in the time course of deactivation when the holding potential was changed (Fig. 1C). The slow activation of the Ca^{2+} current at hyperpolarized potentials (−90 and −60 mV) may be due to the gating current and is explained by a sequential model in which the channel passes through several closed states before the open state (Armstrong, 1981). To explore the voltage-dependent inactivation of the Ca^{2+} current, it was measured by maintaining the neurones for 15 s at a defined holding potential (from −90 to 0 mV). A test pulse to 30 mV was then applied for 5 ms, and the membrane was again repolarized to the holding potential. The maximal amplitude was obtained at −50 mV (Fig. 1D). At holding potentials between −90 and −50 mV, the Ca^{2+} current amplitude showed a small reduction (10 % at −90 mV), probably due to a slow inactivation. The Ca^{2+} current amplitude was constant between −50 and −35 mV, whereas it was abruptly reduced between −30 and 0 mV (Fig. 1D). All these results indicate that the Ca^{2+} current in crayfish XO neurones is generated by HVA Ca^{2+} channels.

Steady-state activation

Although P-type Ca^{2+} currents have been reported in invertebrate preparations (Llinás et al., 1989; Fossier et al., 1994; Hong and Lnenicka, 1997), no kinetic analysis of such currents has been performed in crustacean neurones. To characterize the biophysical properties of the Ca^{2+} current (I_{Ca}) in the XO neurones, a kinetic analysis was performed according to the model of Hodgkin and Huxley (1952) for Na^+ and K^+ currents in squid axon:

$$I_{Ca}(V, t) = I_{Ca,max}(V)m^x(V, t)\,, \quad (1)$$

where $I_{Ca,max}(V)$ is the maximal Ca^{2+} current as a function of voltage (V), x is a constant integer, t is time, and $m(V, t)$ is a

continuous variable from 0 to 1. The term $m^x(V, t)$ reflects the fraction of Ca^{2+} conductance as a function of voltage and time, and is described by:

$$\frac{dm(V,t)}{dt} = \alpha_m(1-m) - \beta_m m = \frac{(m_\infty - m)}{\tau_m}, \quad (2)$$

where α_m and β_m are the first-order rate constants governing the opening and closing of the channel, respectively, $m_\infty=\alpha_m/[\alpha_m(V)+\beta_m(V)]$ is the steady-state value of m, and the time constant $\tau_m=1/[\alpha_m(V)+\beta_m(V)]$.

In the steady state, the fraction of Ca^{2+} conductance (m_∞^x) can be estimated by measuring the tail current amplitude on repolarization to −60 mV after a 5 ms activating pulse. This time allowed full activation of the Ca^{2+} current, with minimal contamination by other currents. The steady-state activation curve has a sigmoidal form (Fig. 2A) and was fitted by the Boltzmann expression:

$$m_\infty^x(V) = 1/\{1 + e^{[(V_{1/2}-V)/V_K]}\}^x, \quad (3)$$

where the mid-point voltage ($V_{1/2}$) was −7.45 mV, the steepness factor (V_K) was 12.04 mV and x=2.

Open-channel current–voltage relationship

To determine the membrane permeability to Ca^{2+}, the instantaneous *I–V* relationship was constructed by measuring the tail current amplitudes at various return potentials (from −60 to 0 mV) after activating a constant number of Ca^{2+} channels at 60 mV from a holding potential of −70 mV. The pulse protocol is illustrated in the Fig. 2B. For voltages higher than 0 mV, the current amplitudes obtained from the *I–V* curves were scaled by matching to the tail current amplitude at 0 mV. The averaged instantaneous *I–V* relationship (Fig. 2C) showed that, even at potentials up to 80 mV, outward currents were not detected. The strong rectification of the instantaneous *I–V* relationship at positive potentials is expected for a highly asymmetric distribution of calcium ions. The continuous line corresponds to the Goldman–Hodgkin–Katz constant-field equation (Goldman, 1943; Hodgkin and Katz, 1949), assuming a single permeant ion:

$$I_{Ca} = P_{Ca}\frac{z^2VF^2}{\boldsymbol{R}T}\frac{a_i - a_o e^{-zVF/\boldsymbol{R}T}}{1 - e^{-zVF/\boldsymbol{R}T}}, \quad (4)$$

where a_o and a_i are the activities of Ca^{2+} outside and inside the cell, P_{Ca} is the permeability of Ca^{2+}, z is the valence, V is the membrane potential, F is Faraday's constant, $\boldsymbol{R}$ is the gas constant and T is absolute temperature. The activities of Ca^{2+} were replaced by their concentrations (5 mmol l^{-1} Ca^{2+} outside and 10 nmol l^{-1} Ca^{2+} inside). The permeation parameter was adjusted to fit the results in Fig. 2C, giving a value of 4.95×10^{-5} cm s^{-1}.

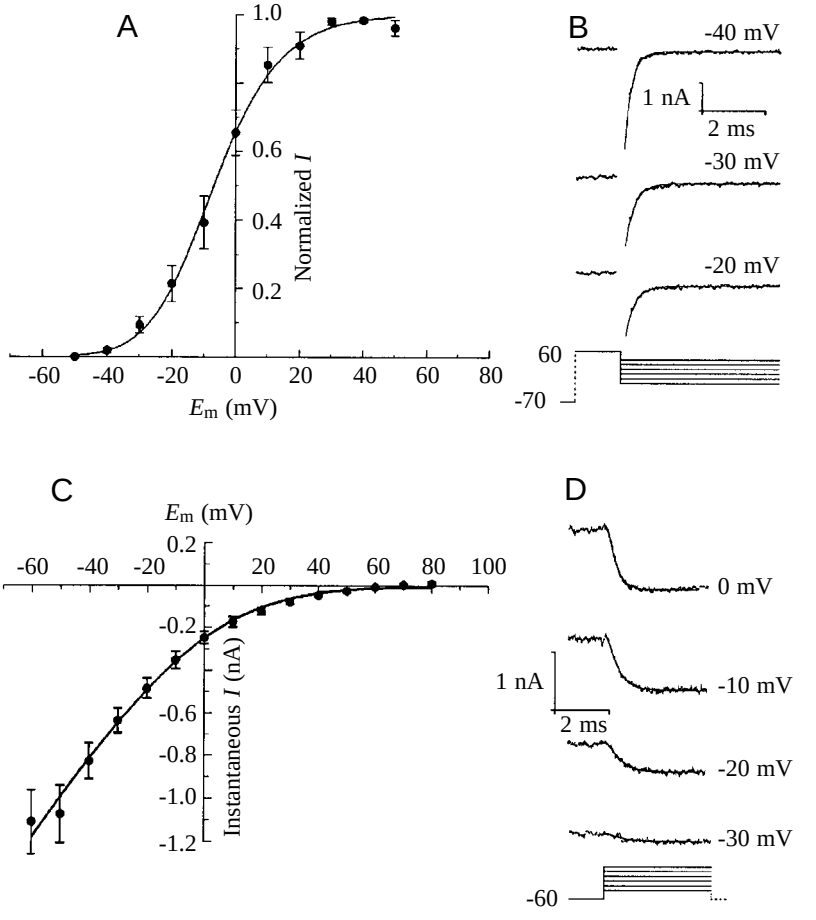

Fig. 2. Steady-state activation and instantaneous current–voltage relationship of the Ca^{2+} current. (A) Averaged steady-state activation curve fitted with the Boltzmann equation (equation 3; see text). Mean ± S.D. from five neurones. (B) Tail Ca^{2+} currents obtained from a holding potential of −70 mV in response to the depolarizing pulses indicated. The traces were fitted with a first-order exponential function. (C) Averaged instantaneous current–voltage relationship from five neurones, fitted with the constant-field equation (equation 4; see text). (D) Onset of the Ca^{2+} current obtained from a holding potential of −60 mV in response to depolarizing command pulses at the values indicated. The superimposed traces were fitted with equation 5 (see text). E_m, membrane potential; I, current.

Activation and inactivation kinetics

The activation of the Ca^{2+} current followed a sigmoidal time course with a variable delay in response to depolarizing pulses (Fig. 2D). The contributions of gating currents, which dominate the earlier part of the activation, were minimized by subtracting the corresponding responses in the presence of 1 mmol l^{-1} Cd^{2+}.

The turn-on kinetics of the Ca^{2+} current, in response to a voltage step, was described by the solution of equation 2:

$$m^x(V, t) = [m_\infty - (m_\infty - m_0)e^{-t/\tau_m(V)}]^x, \quad (5)$$

where m_0 is the value of m at time zero. The currents evoked by voltage steps were fitted by varying x from 1 to 4 and over the range −40 to 40 mV. The expression that best fitted the activation time course of Ca^{2+} currents, at different test potentials, took the m^2 form (Fig. 2D). The time constants (τ_m) obtained using this method were dependent on the test potential and had a maximum value at approximately −20 mV (Fig. 3A).

According to m^2 kinetics, equation 5 implies that the tail current should decay with a single-exponential time course, having a time constant of $0.5\tau_m$, for holding potentials where the steady-state value of m is zero. The time course of the tail current evoked under these conditions was used to estimate the voltage-dependence of τ_m for voltages below −20 mV (Fig. 3A). At more positive potentials, tails could also be fitted by a single-exponential function with a time constant (τ_f) using the expression derived by Hagiwara and Ohmori (1982):

$$\tau_f \approx \tau_m(m_\infty + m_0)/2m_0. \quad (6)$$

Thus, the values of τ_m can be derived from those of τ_f, and the calculated time constants are consistent with the model derived from the turn-on kinetics, suggesting that the derived kinetic model can account for both the activation and deactivation kinetics. The activation time constants, τ_m, estimated from activation and deactivation measurements, show a bell-shaped dependence on membrane potential (Fig. 3A), as expected for a voltage-gated channel.

The rate constants α_m and β_m were then derived from the measured values of m_∞ and τ_m using equations 2 and 5. The rate constants as a function membrane potential (Fig. 3B) were fitted by:

$$\alpha_m(V) = 0.087(-24.72 - V)/[1 - e^{(-24.72-V)/7.74}], \quad (7)$$

$$\beta_m(V) = 0.282(V + 68.93)/[1 - e^{(V+68.93)/17.78}], \quad (8)$$

where α_m and β_m are in ms^{-1} and V is the membrane potential in mV.

Ca^{2+}-dependent inactivation

In voltage-clamped crustacean neurones, as in other preparations, Ca^{2+} currents evoked by depolarizing pulses gradually decay from an initial peak as a result of Ca^{2+} channel inactivation (Hagiwara and Byerly, 1981; Richmond et al., 1995; Branchaw et al., 1997). The extent of inactivation was manifested by a decrease of the tail current amplitude on repolarization following command pulses of various durations

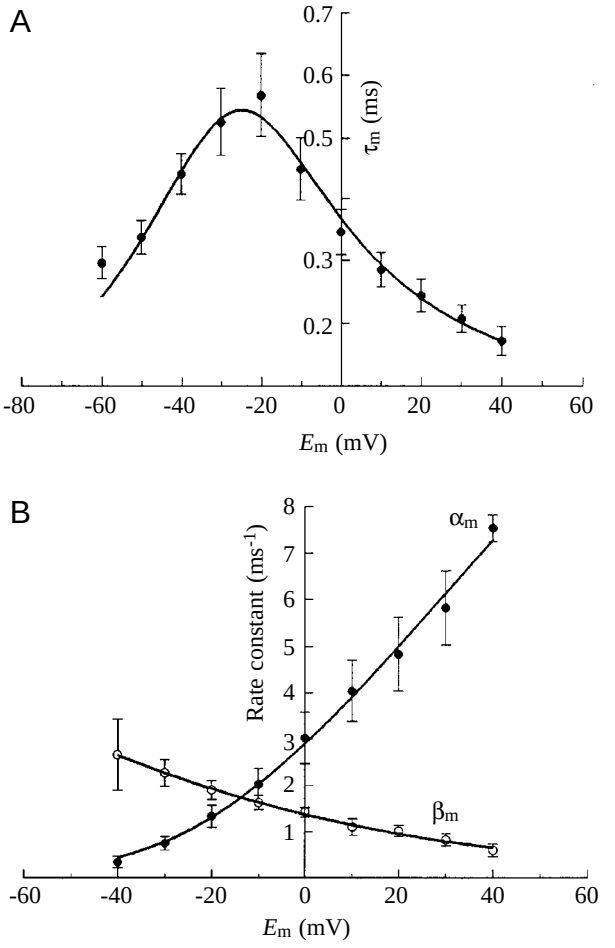

Fig. 3. Activation kinetics of the Ca^{2+} current in XO neurones. (A) The time constant of activation for the m^2 model as a function of voltage derived from the turn-on and turn-off of the Ca^{2+} currents (mean ± S.D. N=5). The time constants from tail currents were obtained by fitting a first-order exponential function. The solid line is given by $\tau_m=1/[\alpha_m(V)+\beta_m(V)]$. (B) Rate constants of activation for the m^2 model. α_m (filled circles) and β_m (open circles) as a function of membrane potential (E_m). Data were calculated from equation 2, using the steady-state activation curve (Fig. 2A) and the time constant data from A. The solid lines are given by equations 7 and 8. τ_m, time constant; α_m, β_m, rate constants. See text for further explanation.

(Fig. 4A), which bears a close relationship with the time course of decay of the Ca^{2+} current.

Moreover, the time course of the decay of the Ca^{2+} current depends on the cation that carries the current. Fig. 4B shows three representative recordings obtained from the same neurone, in which the inward current was carried by Ca^{2+}, Sr^{2+} or Ba^{2+}. When the current was carried by Ba^{2+}, it did not decay during the command pulse, while the Sr^{2+} current decayed more slowly than the Ca^{2+} current, suggesting that Sr^{2+} partially inactivated Ca^{2+} channels. These findings strongly support the idea that the inactivation of the Ca^{2+} current in XO neurones is mediated by Ca^{2+}.

To study the Ca^{2+}-dependent inactivation in more detail, the

relationship between Ca^{2+} entry and Ca^{2+} current inactivation was explored using a double-pulse protocol in which the potential of the prepulse varied from −60 to 110 mV and its effects on a fixed test pulse to 30 mV was evaluated (Fig. 4Ci). Representative traces obtained at prepulse values of 0, 30 and 60 mV are illustrated in the Fig. 4Cii (0 mV at the top, 60 mV at the bottom). The *I–V* relationship obtained with the Ca^{2+} current evoked by the prepulse is illustrated in Fig. 4Ciii, and the inactivation curve (Fig. 4Civ) was obtained by plotting the Ca^{2+} current amplitude evoked by the test pulse as a function of prepulse potential. At the prepulse potential at which Ca^{2+} entry was maximal (30 mV), the inactivation of the Ca^{2+} current was also maximal (35 %). These results indicate that the time-dependent inactivation of the Ca^{2+} current in XO neurones is dependent on the entry of Ca^{2+}.

Recovery from inactivation is another mechanism that can be influenced by intracellular Ca^{2+} concentration (Gutnick et al., 1989). To study this process, we evoked the Ca^{2+} current with prepulses to 30 mV, and after a variable interval at the holding potential (−50 mV) a test pulse with the same characteristics was applied. Short prepulses (10 ms) had less effect on the Ca^{2+} current amplitude evoked by the test pulse, reducing it by 25 % when the interpulse interval was 5 ms. A longer (20 ms) prepulse reduced the current amplitude evoked by the second pulse at the same interpulse interval by 40 % (Fig. 4Di,ii). The time courses of the recovery were fitted with single-exponential curves; the time constants were 17±2.6 for a 10 ms prepulse and 31±3.2 ms for a 20 ms prepulses (means ± S.E.M., *N*=4) (Fig. 4Diii). These results suggest that recovery from the inactivation of the Ca^{2+} current in XO neurones is dependent on the intracellular free Ca^{2+} concentration. Similar results have been reported in neurohypophysis terminals where two mechanisms of Ca^{2+} channel inactivation are implicated, one depending on voltage and the other depending on the intracellular free Ca^{2+} concentration (Branchaw et al., 1997).

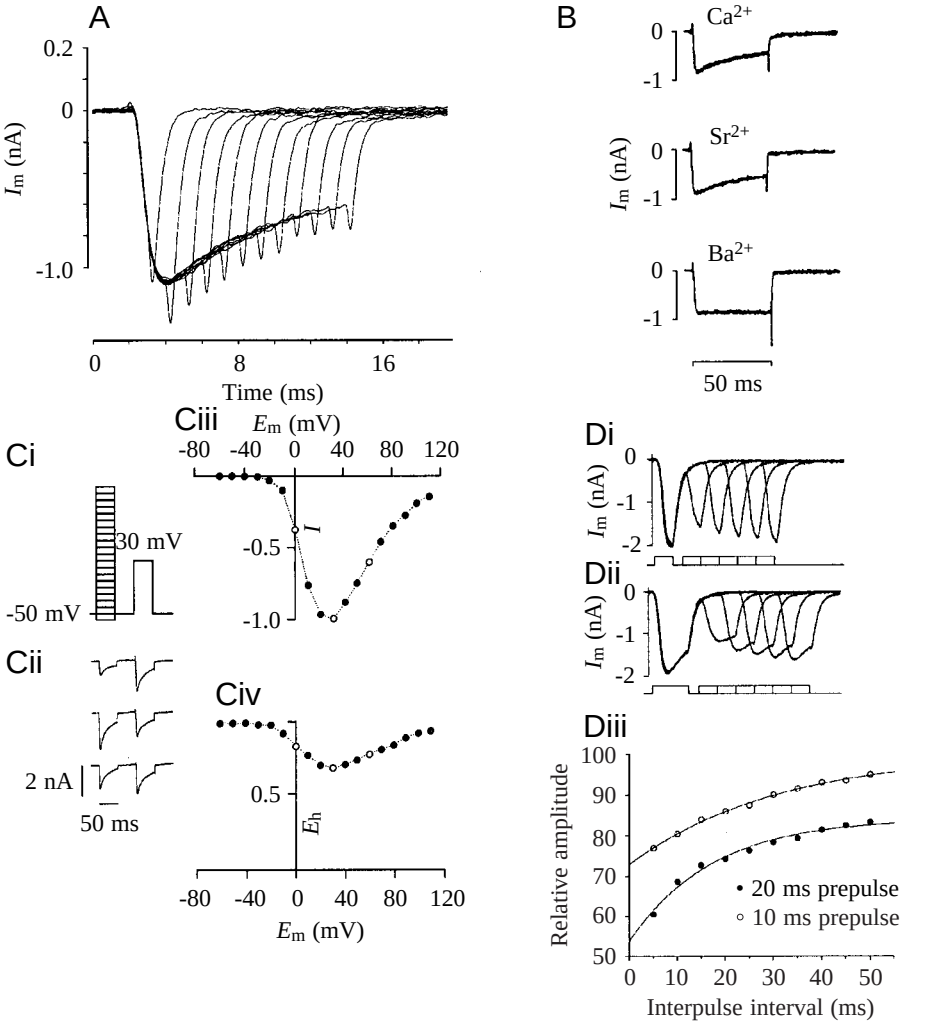

Fig. 4. Ca^{2+}-dependent inactivation and recovery from inactivation of the Ca^{2+} current. (A) Superimposed Ca^{2+} current (I_m) traces recorded from a holding potential of −50 mV in response to a command pulse to 20 mV. The duration of the command pulse was increased progressively in steps of 1 ms. (B) Recordings of Ca^{2+}, Sr^{2+} and Ba^{2+} currents obtained from the same neurone in response to 50 ms depolarizations to 20 mV from a holding potential of −60 mV. The time course of the current decay depended on the divalent cation that carried the current. (C) (i) Double-pulse protocol. Depolarizing prepulses in steps of 10 mV were applied for 50 ms from a holding potential of −50 mV. The membrane was repolarized to the same holding potential for 50 ms, and a test pulse to 30 mV was then applied for 50 ms. (ii) Ca^{2+} current traces that correspond to prepulse values of 0, 30 and 60 mV (from top to bottom). (iii) Normalized current–voltage relationship obtained from the Ca^{2+} current amplitude evoked by the prepulse. *I*, normalized current. (iv) Inactivation curve, the Ca^{2+} current amplitude evoked by the test pulse as a function of the prepulse potential. Current amplitudes were normalized with respect to that evoked in the absence of a prepulse (E_h). (D) The recovery from the inactivation of the Ca^{2+} current depends on previous Ca^{2+} entry. (i) Ca^{2+} current recordings evoked by pairs of depolarizing pulses to 30 mV for 10 ms from a holding potential of −50 mV and separated by variable intervals. (ii) Same protocol as in i, but the duration of the pulses was 20 ms. (iii) The relative current amplitude evoked by the test pulse *versus* the interpulse interval. E_m, membrane potential.

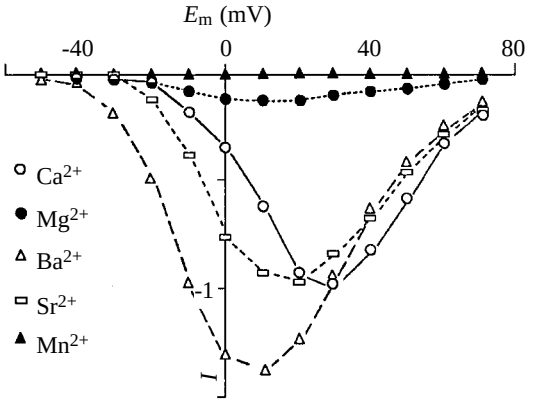

Fig. 5. Divalent cation permeation through Ca^{2+} channels in XO neurones. Typical current–voltage (*I–V*) relationships for different divalent cation currents normalized with respect to the maximal Ca^{2+} current (see text). The concentration of each cation was 13.5 mmol l^{-1}. All the *I–V* relationships were obtained from the same neurone, from a holding potential of −50 mV and with 10 ms depolarizing command pulses. E_m, membrane potential.

Selectivity and blockage by divalent cations

To explore the selectivity sequence of divalent cations through Ca^{2+} channels in XO neurones, extracellular Ca^{2+} (13.5 mmol l^{-1}) was equimolarly replaced by Ba^{2+}, Sr^{2+}, Mg^{2+}, Mn^{2+}, Co^{2+}, Ni^{2+} or Cd^{2+}. In a series of experiments, *I–V* relationships were obtained from a holding potential of −60 mV with 50 ms depolarizing pulses at 10 mV intervals. Ba^{2+}, Sr^{2+} and Mg^{2+} were able to generate currents, but Mn^{2+}, Co^{2+}, Ni^{2+} and Cd^{2+} failed to generate currents (Fig. 5; results for Co^{2+}, Ni^{2+} and Cd^{2+} not shown). The selectivity sequence for permeable divalent cations was 1.4 (Ba^{2+}), 1.0 (Sr^{2+}) and 0.2 (Mg^{2+}). These values were obtained by normalizing the current carried by any one of the divalent cations with respect to the maximal Ca^{2+} current. The activation threshold of Ba^{2+} and Sr^{2+} currents was shifted in the hyperpolarizing direction by 20 mV, and the maximum current values were shifted in the hyperpolarizing direction by 10 V, in comparison with the activation threshold of the Ca^{2+} current.

Blocking of the Ca^{2+} current in XO neurones by divalent cations was explored by superfusing Co^{2+}, Ni^{2+}, Cd^{2+} or Zn^{2+}, at low concentrations, in the presence of the normal Ca^{2+} concentration. Ca^{2+} currents were recorded first in the absence and then in the presence of the blocking ion, from a holding potential of −50 mV with 10 mV depolarizing steps for 50 ms. The Ca^{2+} current was more effectively blocked by Cd^{2+} and Zn^{2+} than by Co^{2+} and Ni^{2+} (Fig. 6A). The maximal blocking effect on the Ca^{2+} current of Zn^{2+} or Cd^{2+} (100 μmol l^{-1}) averaged 80 %, and the effects were partially reversible. Blockage by Ni^{2+} or Co^{2+} (2 mmol l^{-1}) was less effective (40 %). Furthermore, the block caused by Co^{2+} and Cd^{2+} was less potent at negative potentials, whereas the opposite was true for Ni^{2+} and Zn^{2+} (Fig. 6B), suggesting a voltage-dependent mechanism.

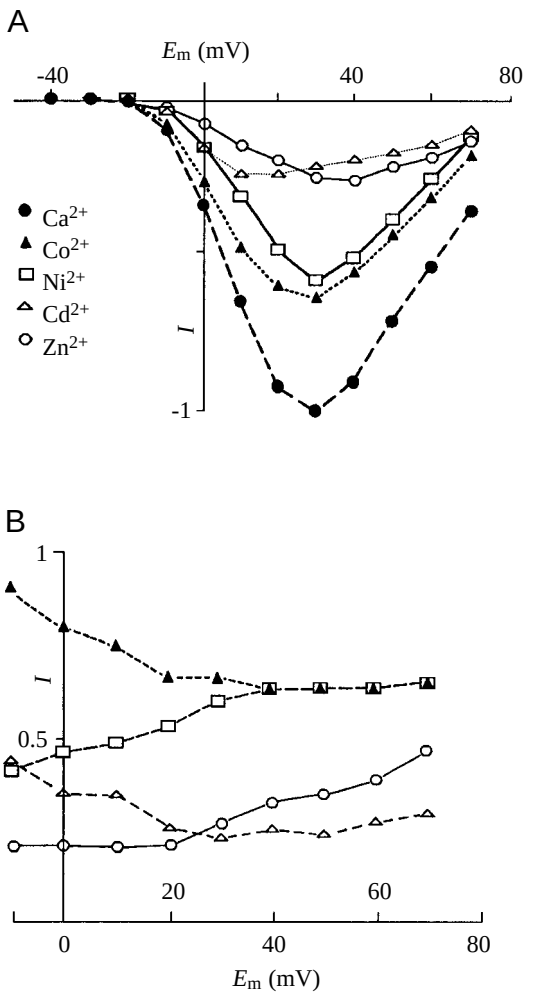

Fig. 6. Blockage of the Ca^{2+} current by divalent cations. (A) Representative current–voltage (*I–V*) curves normalized to the averaged *I–V* relationship of the control Ca^{2+} current. After obtaining the control *I–V* curve, Co^{2+} (2 mmol l^{-1}), Ni^{2+} (2 mmol l^{-1}), Cd^{2+} (100 μmol l^{-1}) or Zn^{2+} (100 μmol l^{-1}) was added to the external solution. The reduction in the amplitude of the Ca^{2+} current shows the extent of blockage produced by these cations. Depolarizing pulses (10 mV, 10 ms) were applied from a holding potential of −50 mV. (B) The resistant fraction of the Ca^{2+} current plotted against the membrane potential (E_m) (data from A). The blockage of the Ca^{2+} current exerted by these cations was voltage-dependent.

Pharmacology

To explore the pharmacological properties of the Ca^{2+} current and to identify the possible multiple components of HVA Ca^{2+} channels involved in generating the Ca^{2+} current, we performed a series of experiments in which we applied several derivatives of DHPs, such as nitrendipine, nifedipine, nimodipine or Bay K-8644, as well as derivatives of phenylalkylamines, such as verapamil or D-600. None of these compounds, applied extracellularly at concentrations up to 20 μmol l^{-1}, affected the Ca^{2+} current.

The Ca^{2+} current was blocked by the P-type Ca^{2+}-channel-selective peptide ω-agatoxin-IVA at a low extracellular Ca^{2+} concentration (5 mmol l^{-1}). Fig. 7A illustrates the effect of

200 nmol l^{-1} ω-agatoxin-IVA on the amplitude of the Ca^{2+} current. In three neurones, the Ca^{2+} current amplitude was rapidly reduced by 85 % by the toxin to reach a maximal level of block at approximately 1 min; the block persisted after the peptide had been washed out. However, when two or three trains of depolarizing pulses (2 ms) to 60 mV at 5 Hz were applied for 5 s, after the maximal effect of the toxin, the blockage was partially removed, 80 % of the Ca^{2+} current amplitude being recovered (Fig. 7A), suggesting that the effects exerted by the toxin are voltage-dependent, as has been reported previously in vertebrate neurones (Mintz et al., 1992). The degree of block was dependent on the toxin concentration, 50 and 100 nmol l^{-1} reduced the Ca^{2+} current amplitude by 10 and 35 %, respectively. In contrast, at the normal extracellular Ca^{2+} concentration, the peptide was ineffective in blocking the current at concentrations up to 500 nmol l^{-1}. Other peptide toxins specific for N-type (ω-conotoxin-GVIA, 2 µmol l^{-1}) and Q-type (ω-conotoxin-MVIIC, 5 µmol l^{-1}) Ca^{2+} channels had no effect on the Ca^{2+} current in XO neurones (Fig. 7B,C).

Finally, when the fraction of Ca^{2+} current resistant to ω-agatoxin-IVA (Fig. 8A) was scaled up to match the control recording, we observed that the kinetics of activation and deactivation were the same (Fig. 8C). The transient outward current at the beginning of the pulse (gating current) was not affected by the toxin. Furthermore, the residual Ca^{2+} current showed an *I–V* relationship with the same characteristics as the control Ca^{2+} current: the same threshold for activation and a maximum value at 20 mV (Fig. 8B). These results suggest that crayfish XO neurones express a single class of P-type Ca^{2+} channels.

Discussion

When the Ca^{2+} current is activated, other physiological events such as action potentials occur, with the entry of Ca^{2+} participating in the firing pattern (Meyers et al., 1992). This phenomenon is probably important in neurosecretory cells, since during normal electrical activity Ca^{2+} channels are activated and allow the influx of Ca^{2+}, a process crucial for cellular functions such as the inactivation of the Ca^{2+} channels themselves, the modulation of K^+ channels (Martínez et al., 1991; Onetti et al., 1996), participation in the negative slope

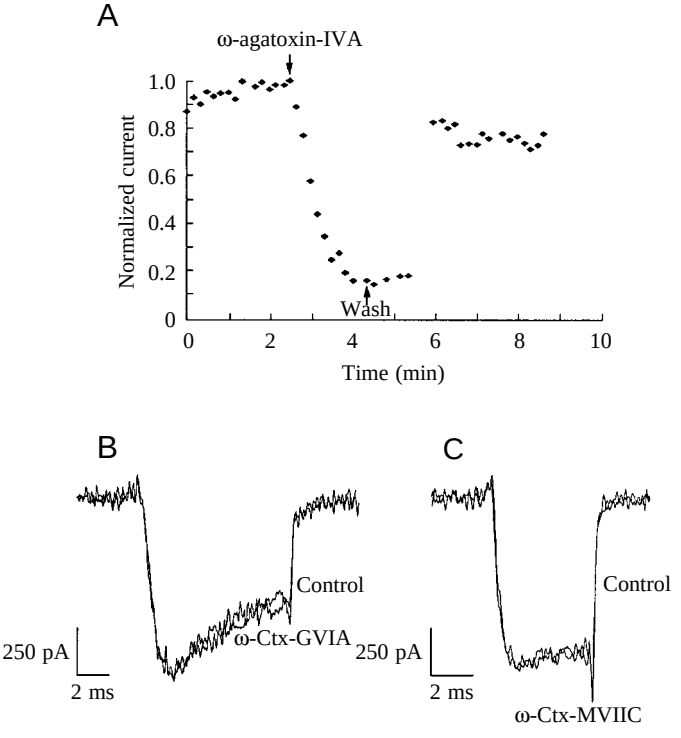

Fig. 7. Pharmacological features of the Ca^{2+} current in crayfish XO neurones. (A) Plot of the Ca^{2+} current amplitude against time. Ca^{2+} currents were evoked by depolarizing command pulses to 30 mV for 5 ms, from a holding potential of −50 mV at a frequency of 0.1 Hz. When the current amplitude was stable, the toxin was superfused; its application (at 200 nmol l^{-1}) and removal are indicated by arrows. (B,C) Superimposed Ca^{2+} current traces obtained before and after the application of 2 µmol l^{-1} ω-conotoxin-GVIA (ω-Ctx-GVIA) or 5 µmol l^{-1} ω-conotoxin-VIIC (ω-Ctx-VIIC). These peptide toxins did not modify the amplitude or the time course of the Ca^{2+} current.

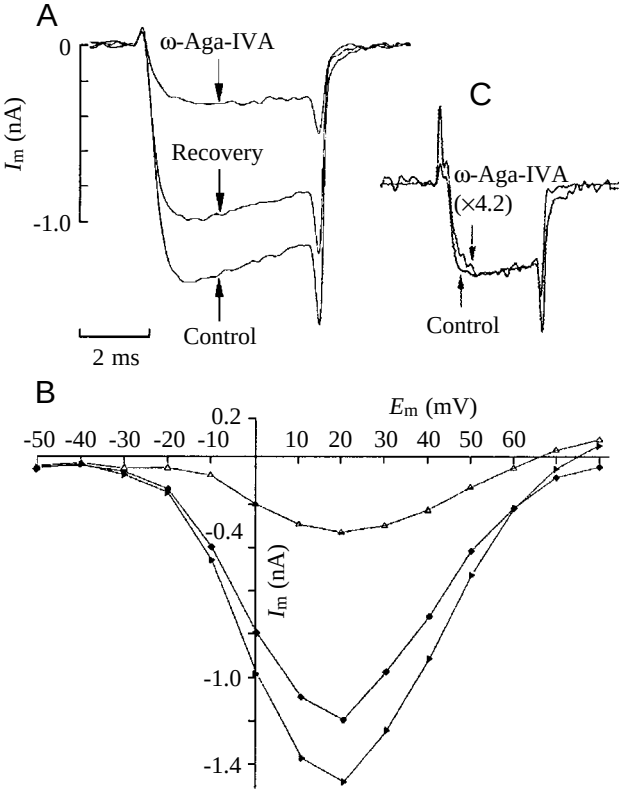

Fig. 8. Effects of 200 nmol l^{-1} ω-agatoxin-IVA (ω-Aga-IVA) on the Ca^{2+} current. (A) Ca^{2+} current (I_m) traces obtained before, during and after toxin application. The command pulse protocol was the same as in Fig. 7. (B) Current–voltage (*I–V*) relationships obtained from the same neurone, before (filled triangles), during (open triangles) and after (filled diamonds) the application of toxin. The experimental protocol was the same as in Fig. 6. (C) The current resistant to the toxin was scaled up (×4.2) to compare its shape with that of the control current.

conductance (Onetti et al., 1990) and neuropeptide secretion (Renaud, 1988; Wang et al., 1997).

LVA Ca^{2+} currents seem to be absent in crayfish XO neurones because (a) the inactivation and deactivation kinetics of the Ca^{2+} current could be fitted to single-exponential functions, (b) the *I–V* relationship did not have an additional peak at hyperpolarized potentials values and (c) the Ca^{2+} tail current amplitude did not change when it was evoked from different holding potentials (see Fig. 1C). Similar results have been reported in XO neurones from the crab *Cardisoma carnifex* (Richmond et al., 1995).

Activation of the Ca^{2+} current has been described in a variety of preparations using the Hodgkin and Huxley model (m^x), in which the exponent x accounts for the speed of the activation (Adams and Gage, 1979; Llinás et al., 1981; Sala, 1991). In the present study, the onset of the Ca^{2+} current clearly follows the predicted kinetics at all the potentials tested. Additionally, the tail current data are consistent with the kinetics, implying a linear sequential model with two closed states and one open state. The Ca^{2+} current in XO neurones activates in a similar manner to that in in pituitary cells (Hagiwara and Ohmori, 1982) and in sympathetic and hippocampal neurones (Belluzzi and Sacchi, 1989; Kay and Wong, 1987; Sala, 1991). According to the model, the predicted mean open time of the Ca^{2+} channel at −20 mV would be 568 μs, a value faster than that in sympathetic neurones (Sala, 1991) and in chromaffin cells (Fenwick et al., 1982).

The small reduction of the Ca^{2+} current amplitude evoked from holding potentials between −90 and −35 mV does not appear to be due to inactivation, because tail current amplitudes and their time courses were identical for three different holding potentials (Fig. 1C), indicating that the number of channels that remained open at the time of repolarization was the same in the three cases. An explanation for this reduction may be the presence of an outward gating current superimposed on Ca^{2+} current activation, the presence of another type of Ca^{2+} channel that inactivates slightly in this voltage range or a very slow inactivation of the Ca^{2+} channels. To differentiate between these, it will be necessary to explore this process in more detail.

The time-dependent decay of the Ca^{2+} current during depolarizing command pulses could be due to (a) depletion of extracellular Ca^{2+}, (b) contamination with outward currents, or (c) inactivation of Ca^{2+} channels. The first two possibilities were rejected because no effects were observed on the time course of the Ca^{2+} current when the cells were continuously superfused with a solution containing 13.5 mmol l^{-1} Ca^{2+} or when Cl^- was replaced with $CH_3SO_4^-$ or Cs^+ was replaced with TMA^+. The decay of the Ca^{2+} current in XO neurones is therefore probably due to the inactivation of Ca^{2+} channels. At least two mechanisms have been described for inactivating the Ca^{2+} current, one that depends on membrane potential and another that depends on $[Ca^{2+}]_i$ (Chad and Eckert, 1984). An increase in intracellular free Ca^{2+} concentration favours the inactivation of Ca^{2+} channels in a variety of preparations (Ashcroft and Stanfield, 1982; Gutnick et al., 1989; Plant et al., 1983). It appears that the mechanism of inactivation of the Ca^{2+} current in XO neurones is mediated mainly by Ca^{2+}. This is supported by the observation that the current carried by Ba^{2+} did not decay, at least during the 50 ms command pulses, and that the amplitude of the Ca^{2+} current depended on previous influx of Ca^{2+}, as in other crustacean peptidergic neurones (Meyers et al., 1992; Richmond et al., 1995). The U-shaped curve obtained from a double-pulse protocol (Fig. 4Civ) is a hallmark of Ca^{2+}-dependent inactivation (Chad and Eckert, 1984) and is due to accumulation of Ca^{2+} in a submembrane compartment, probably binding to the open Ca^{2+} channels.

In a variety of cells, Ba^{2+} is more effective as a charge carrier than Ca^{2+}, probably because of its lower affinity for the channel (Hagiwara and Byerly, 1981). On the basis of the peak current for the *I–V* relationships with different divalent cations, the selectivity sequence in crayfish XO neurones was: $Ba^{2+}>Sr^{2+}\approx Ca^{2}\gg Mg^{2+}$, in comparison with crab peptidergic neurones, in which the reported sequence was $Ba^{2+}>Sr^{2+}>Ca^{2+}$ (Richmond et al., 1995). The shift of the *I–V* relationship of the Ba^{2+} current may be explained because Ba^{2+} is less effective than Ca^{2+} in shielding the membrane charge (Frankenhaeuser and Hodgkin, 1957). Other divalent cations that act as Ca^{2+} channel blockers (Mn^{2+}, Co^{2+}, Ni^{2+} and Cd^{2+}) can also carry inward current through Ca^{2+} channels (for a review, see Hagiwara and Byerly, 1981). However, in crayfish XO neurones, we found that these cations did not generate currents, as they do in other crustacean neurones (Meyers et al., 1992; Richmond et al., 1995).

Blockage of the Ca^{2+} current in XO neurones by the divalent cations tested here depended on their concentration and on the membrane potential. We found that Cd^{2+} and Zn^{2+} were more effective in blocking the Ca^{2+} current than Co^{2+} and Ni^{2+}, suggesting that they have a higher affinity for the Ca^{2+} channel than do Co^{2+} and Ni^{2+}. In contrast, Ni^{2+} and Zn^{2+} blocked the Ca^{2+} current more effectively at hyperpolarized values (−10 to 50 mV), whereas block of the Ca^{2+} current by Co^{2+} and Cd^{2+} was more effective at depolarizing potentials (30–70 mV). The voltage-dependence of Ca^{2+} current blockage by divalent cations suggests that they interact within the ion channel. Thus, two additional criteria indicate that the inward Ca^{2+} current in XO neurones is generated by HVA channels: (a) the permeability to Ba^{2+} was higher than that to Ca^{2+} and (b) the blockage exerted by Cd^{2+} was greater than that exerted by Ni^{2+} (Tsien et al., 1988).

Dihydropyridines (DHPs), at concentrations of 10 μmol l^{-1}, block nearly all L-type Ca^{2+} current in ventricular myocytes and photoreceptors (Barnes and Hille, 1989; Balke et al., 1992). However, DHPs (nitrendipine, nifedipine, nimodipine or Bay K-8644) at concentrations of 20 μmol l^{-1} and phenylalkylamines (verapamil or D-600) at concentrations of 20 μmol l^{-1} had no effect on the Ca^{2+} current, indicating that the crayfish XO neurones do not express an L-type Ca^{2+} current.

One common feature of L-, N-, P-, Q- and R-type currents is their activation over the same range of membrane potentials, and it is difficult to distinguish them by their kinetics,

permeability and blockage by inorganic cations (Usowics et al., 1992). Thus, the identification of HVA Ca^{2+} currents is based mainly on pharmacological tests. In the XO neurone somata, relatively high concentrations of ω-agatoxin-IVA (200 nmol l^{-1}) blocked 85 % of the total Ca^{2+} current. These results suggest that the Ca^{2+} channels expressed in XO neurones share the pharmacological properties of P-type Ca^{2+} channels, with less specificity for ω-agatoxin-IVA than the Ca^{2+} channels of mammalian neurones (Brown et al., 1994; Llinás et al., 1992; Mintz et al., 1992). For instance, in cerebellar Purkinje neurones, ω-agatoxin-IVA has a high selectivity for P-type Ca^{2+} channels with a dissociation constant K_d of 2–10 nmol l^{-1} (Mintz et al., 1992). However, in the marine crab *Cardisoma carnifex*, high concentrations of ω-agatoxin-IVA (500 nmol l^{-1}) did not affect the Ca^{2+} current or peptide release in either freshly dissociated XO neurones (Richmond et al., 1995) or peptidergic terminals (Richmond et al., 1996), even at the low extracellular Ca^{2+} concentration at which the toxin appears to be more effective. In contrast, transmitter release at the neuromuscular junction (Araque et al., 1994) and the Ca^{2+} current in motoneurones (Hong and Lnenicka, 1997) from the freshwater crayfish are affected by concentrations of ω-agatoxin-IVA between 30 and 600 nmol l^{-1}. In the present study, the Ca^{2+} current in crayfish XO neurones was blocked by ω-agatoxin-IVA at a low extracellular Ca^{2+} concentration (5 mmol l^{-1}); at a normal extracellular Ca^{2+} concentration (13.5 mmol l^{-1}), ω-agatoxin-IVA was ineffective. *Cardisoma carnifex* XO neurones, in which peptide toxins have no effect on the Ca^{2+} current, may express R-type Ca^{2+} channels differing from the Ca^{2+} channels expressed in the crayfish XO neurones, which appear to be P-type Ca^{2+} channels.

Recently, R. Alvarado-Alvarez, E. Becerra and U. García (in preparation) have suggested that the P-type Ca^{2+} current participates in secretory activity, and they have developed a sensitive bioassay to demonstrate this. Their assay is based on the pigmentary matrix retraction of erythrophores cultured together with identified XO neurones that produce red pigment concentrating hormone. Both neuronal Ca^{2+} currents, evoked by depolarizing command pulses, and neuronal firing, induced by depolarizing current injection, were able to induce aggregation on the target cells.

We discounted the existence of N- and Q-type Ca^{2+} channels in crayfish XO neurones because ω-conotoxin-GVIA, which acts selectively on N-type Ca^{2+} channels, did not affect the magnitude or the time course of the Ca^{2+} current in these neurones (Fig. 7B,C). Furthermore, the Q-type channel is resistant to low doses of ω-agatoxin-IVA (30 nmol l^{-1}), but is sensitive to micromolar concentrations of ω-conotoxin-MVIIC (Ellinor et al., 1993), whereas the opposite occurs in XO neurones.

These results do not exclude the existence of R-type Ca^{2+} channels in crayfish XO neurones, since 15 % of the total Ca^{2+} current was resistant to ω-agatoxin-IVA, even at 500 nmol l^{-1}. We suggest that the remaining current could be similar to that described in crab XO neurones (Richmond et al., 1995).

We thank Leopoldo Gonzalez Santos and Benita Mendiola for valuable technical assistance. U.G. was supported by CONACyT grant 1402-N9206.

References

Adams, D. J. and Gage, P. W. (1979). Characteristics of sodium and calcium conductance changes produced by membrane depolarization in an *Aplysia* neurone. *J. Physiol., Lond.* **289**, 143–161.

Almers,W., Stanfield, P. R. and Stühmer, W. (1983). Lateral distribution of sodium and potassium channels in frog skeletal muscle: measurements with a patch-clamp technique. *J. Physiol., Lond.* **336**, 261–284.

Angstadt, J. D. and Calabrese, R. L. (1991). Calcium currents and graded synaptic transmission berween heart interneurons of the leech. *J. Neurosci*. **11**, 746–759.

Aosaki, T. and Kasai, H. (1989). Characterization of two kinds of high-voltage-activated Ca-channel currents in chick sensory neurons: Differential sensitivity to dihydropyridines and ω-conotoxin GVIA. *Pflügers Arch.* **414**, 150–156.

Araque, A., Clarac, F. and Bruño, W. (1994). P-type Ca^{2+} channels mediate excitatory and inhibitory synaptic transmitter release in crayfish muscle. *Proc. Natl. Acad. Sci. USA* **91**, 4224–4228.

Armstrong, C. M. (1981). Sodium channels and gating currents. *Physiol. Rev*. **61**, 644–683.

Ashcroft, F. M. and Stanfield, P. R. (1982). Calcium inactivation in skeletal muscle fibers of the stick insect *Carausius morosus*. *J. Physiol., Lond.* **330**, 349–372.

Balke, C. W., Rose, W. C., Marban, E. and Wier, W. G. (1992). Macroscopic and unitary properties of physiological ion flux through T-type Ca^{2+} channels in guinea-pig heart cells. *J. Physiol., Lond.* **456**, 247–265.

Barnes, S. and Hille, B. (1989). Ionic channels of the inner segment of tiger salamander cone photoreceptors. *J. Gen. Physiol*. **94**, 719–743.

Belluzzi, O. and Sacchi, O. (1989). Calcium currents in the normal adult rat sympathetic neurone. *J. Physiol., Lond.* **412**, 493–512.

Branchaw, J. L., Banks, M. I. and Jackson, M. B. (1997). Ca^{2+}- and voltage-dependent inactivation of Ca^{2+} channels in nerve terminals of the neurohypophysis. *J. Neurosci*. **17**, 5772–5781.

Brown, A. M., Sayer, R. J., Schwindt, P. C. and Crill, W. E. (1994). P-type calcium channels in rat neocortical neurones. *J. Physiol., Lond.* **475**, 197–205.

Carbone, E. and Lux, H. D. (1984). A low voltage activated, fully inactivating Ca^{2+} channel in vertebrate sensory neurones. *Nature* **310**, 501–502.

Chad, J. E. and Eckert, R. (1984). Calcium ‘domains‘ associated with individual channels may account for anomalous voltage relations of Ca-dependent responses. *Biophys. J.* **45**, 993–999.

Coulter, D. A., Huguenard, J. P. and Prince, D. A. (1989). Characterization of ethosuximide reduction of low-threshold calcium current in thalamic neurons. *Ann. Neurol*. **25**, 582–593.

Ellinor, P. T., Zhang, J. F., Randall, A. D., Zhou, M., Schwarz, T. L., Tsien, R. W. and Horne, W. A. (1993). Functional expression of a rapidly inactivating neuronal calcium channel. *Nature* **363**, 455–458.

Fenwick, E. M., Marty, A. and Neher, E. (1982). Sodium and calcium channels in bovine chomaffin cells. *J. Physiol., Lond.* **331**, 599–635.

Fossier, P., Baux, G. and Tauc, L. N. (1994). P-type Ca^{2+} channels

are involved in acetylcholine release at a neuronal synapse: only the N-type channel is the target of neuromodulators. *Proc. Natl. Acad. Sci. USA* **91**, 4771–4775.

Fox, A. P., Nowycky, M. C. and Tsien, R. W. (1987). Kinetics and pharmacological properties distinguishing three types of calcium currents in chick sensory neurones. *J. Physiol., Lond.* **394**, 149–172.

Frankenhaeuser, B. and Hodgkin, A. L. (1957). The action of calcium on the electrical properties of squid axons. *J. Physiol., Lond.* **137**, 218–244.

García, U., Grumbacher-Reinert, S., Bookman, R. and Reuter, H. (1990). Distribution of Na^+ and K^+ currents in soma, axons and growth cones of leech Retzius neurones in culture. *J. Exp. Biol.* **150**, 1–17.

Goldman, D. E. (1943). Potential, impedance and rectification in membranes. *J. Gen. Physiol*. **27**, 37–60.

Gutnick, M. J., Lux, H. D., Swandulla, D. and Zucker, H. (1989). Voltage-dependent and calcium-dependent inactivation of calcium channel current in identified snail neurones. *J. Physiol., Lond.* **412**, 197–220.

Hagiwara, S. and Byerly, L. (1981). Calcium channel. *Annu. Rev. Neurosci*. **4**, 69–125.

Hagiwara, S. and Ohmori, H. (1982). Studies of calcium channels in rat clonal pituitary cells with patch electrode voltage clamp. *J. Physiol., Lond.* **331**, 231–252.

Haydon, P. G. and Man-Son-Hing, H. (1988). Low- and high-voltage-activated calcium currents: their relationship to the site of neurotransmitter release in an identified neuron of *Helisoma. Neuron* **1**, 919–927.

Herrington, J. and Lingle, C. J. (1992). Kinetic and pharmacological properties of low voltage-activated Ca^{2+} current in rat clonal (GH_3) pituitary cells. *J. Neurophysiol*. **68**, 213–232.

Hess, P., Lansman, J. B. and Tsien, R. W. (1984). Different modes of Ca^{2+} channel gating behaviour favoured by dihidropyridine Ca^{2+} agonists and antagonists. *Nature* **311**, 538–544.

Hillyard, D. R., Monje, V. D., Mintz, I. M., Bean, B. P., Nadasdi, L., Ramachandan, J., Miljanich, G., Azimi-Zoonooz, A., McIntosh, J. M., Cruz, L. J., Imperial, J. S. and Olivera, B. M. (1992). A new conus peptide ligand for mammalian presynaptic Ca^{2+} channels. *Neuron* **9**, 69–77.

Hodgkin, A. L. and Huxley, A. F. (1952). A quantitative description of membrane current and its application to conduction and excitation in nerve. *J. Physiol., Lond.* **117**, 500–544.

Hodgkin, A. L. and Katz, B. (1949). The effect of sodium ions on the electrical activity of the giant axon of the squid. *J. Physiol., Lond.* **108**, 37–77.

Hong, S. J. and Lnenicka, G. A. (1997). Characterization of a P-type calcium current in a crayfish motoneuron and its selective modulation by impulse activity. *J. Neurophysiol*. **77**, 76–85.

Iwasaki, S. and Satow, I. (1971). Sodium and calcium-dependent spike potentials in the secretory neurons soma of the X-organ of the crayfish. *J. Gen. Physiol*. **57**, 216–238.

Kasai, H. and Neher, E. (1992). Dihydropyridine-sensitive and ω-conotoxin-sensitive calcium channels in mammalian neuroblastoma-glioma cell line. *J. Physiol., Lond.* **448**, 161–188.

Kay, A. B. and Wong, R. K. S. (1987). Calcium current activation kinetics in isolated pyramidal neurones of the CA1 region of the mature guinea-pig hippocampus. *J. Physiol., Lond.* **392**, 603–616.

Llinás, R., Steinberg, I. Z. and Walton, K. (1981). Presynaptic calcium currents in squid giant synapse. *Biophys. J*. **33**, 289–322.

Llinás, R., Sugimori, M., Hillman, D. E. and Cherksey, B. (1992). Distribution and functional significance of the P-type, voltage-dependent Ca^{2+} channels in the mammalian central nervous system. *Trends Neurosci*. **15**, 351–355.

Llinás, R., Sugimori, M., Lin, J. W. and Cherksey, B. (1989). Blocking and isolation of a calcium channel from neurons in mammals and cephalopods utilizing a toxin fraction (FTX) from funnel-web spider poison. *Proc. Natl. Acad. Sci. USA* **86**, 1689–1693.

Martínez, J. J., Onetti, C. G., García, E. and Hernández, S. (1991). Potassium current kinetics in bursting secretory neurons: effects of intracellular calcium. *J. Neurophysiol.* **66**, 1455–1461.

Meyers, D. E. R., Graf, R. A. and Cooke, I. M. (1992). Ionic currents of morphologically distinct peptidergic neurons in defined culture. *J. Neurophysiol*. **67**, 1301–1315.

Miller, R. J. (1992). Voltage sensitive Ca^{2+} channels. *J. Biol. Chem*. **267**, 1403–1406.

Mintz, I. M., Venema, V. J., Swiderek, K., Lee, T., Bean, B. P. and Adams, M. E. (1992). P-type calcium channels blocked by the spider toxin ω-Aga-IVA. *Nature* **355**, 827–829.

Mori, Y. (1994). Molecular biology of voltage-dependent calcium channels. In *Handbook of Membrane Channels: Molecular and Cellular Physiology* (ed. C. Peracchia), pp. 163–176. San Diego, CA: Academic Press Inc.

Onetti, C. G., García, U., Valdiosera, R. F. and Aréchiga., H. (1990). Ionic currents in crustacean neurosecretory cells. *J. Neurophysiol*. **64**, 1514–1526.

Onetti, C. G., Lara, J. and García, E. (1996). Adenine nucleotides and intracellular Ca^{2+} regulate a voltage-dependent and glucose-sensitive potassium channel in neurosecretory cells. *Pflügers Arch.* **432**, 144–154.

Plant, T. D., Standen, N. B. and Ward, T. A. (1983). The effects of injection of calcium ions and calcium chelators on calcium channel inactivation in *Helix* neurones. *J. Physiol., Lond.* **334**, 189–212.

Plummer, M. R., Logothetis, D. E. and Hess, P. (1989). Elementary properties and pharmacological sensitivities of calcium channels in mammalian peripheral neurons. *Neuron* **2**, 1453–1463.

Randall, A. and Tsien, R. W. (1995). Pharmacological dissection for multiple types of Ca^{2+} channels currents in rat cerebellar granule neurons. *J. Neurosci*. **15**, 2995–3012.

Renaud, L. P. (1988). Electrophysiology of a peptidergic neuron. The hypothalamic magnocellular neurosecretory cell. In *Neurotransmitters and Cortical Function (*ed. M. Avoli, T. A. Reader, R. W. Dykes and O. Gloor), pp. 495–515. New York: Plenum.

Richmond, J. E., Penner, R., Keller, R. and Cooke, I. M. (1996). Characterization of the Ca^{2+} current in isolated terminals of crustacean peptidergic neurons. *J. Exp. Biol*. **199**, 2053–2059.

Richmond, J. E., Sher, E. and Cooke, I. M. (1995). Characterization of the Ca^{2+} current in freshly dissociated crustacean peptidergic neuronal somata. *J. Neurophysiol.* **73**, 2357–2368.

Sala, F. (1991). Activation kinetics of calcium currents in bull-frog sympathetic neurones. *J. Physiol., Lond*. **437**, 221–238.

Sather, W. A., Tanabe, T., Zhang, J. F., Mori, Y., Adams, M. E. and Tsien, R. W. (1993). Distinctive biophysical and pharmacological properties of class A (BI) calcium channel α_1 subunits. *Neuron* **11**, 291–303.

Snutch, T. P. and Reiner, P. B. (1992). Ca^{2+} channels: diversity of form and function. *Curr. Opin. Neurobiol*. **2**, 247–253.

Stuenkel, E. L. (1985). Simultaneous monitoring of electrical and secretory activity in peptidergic neurosecretory terminals of the crab. *J. Physiol., Lond.* **359**, 163–187.

Swandulla, D., Carbone, E. and Lux, H. D. (1991). Do calcium channel classifications account for neuronal calcium channel diversity? *Trends Neurosci*. **14**, 46–51.

Tang, C., Presser, F. and Morad, M. (1988). Amiloride selectively blocks the low threshold (T) calcium channels. *Science* **240**, 213–215.

Tsien, R. W., Lipscombe, D., Madison, D. V., Bley, K. R. and Fox, A. P. (1988). Multiple types of neuronal calcium channels and their selective modulation. *Trends Neurosci*. **11**, 431–438.

Tsien, R. W. and Tsien, R. Y. (1990). Calcium channels, stores and oscillations. *Annu. Rev. Cell Biol*. **6**, 715–760.

Usowicz, M. M., Sugimori, M., Cherksey, B. and Llinás, R. (1992). P-type calcium channels in the somata and dendrites of adult cerebellar Purkinje cells. *Neuron* **9**, 1185–1199.

Wang, G., Dayanithi, G., Kim, S., Hom, D., Nadasdi, L., Kristipati, R., Ramachandran, J., Stuenkel, E. L., Nordman, J. J., Newcomb, R. and Lemos, J. R. (1997). Role of Q-type Ca^{2+} channels in vasopressin secretion from neurohypophysial terminals of the rat. *J. Physiol., Lond.* **502**, 351–363.

Wang, G. and Lemos, J. R. (1994). Effects of funnel web spider toxin on Ca^{2+} currents in neurohypophysial terminals. *Brain Res*. **663**, 215–222.

Zhang, J. F., Randall, A. D., Ellinor, P. T., Horne, W. A., Sather, W. A., Tanabe, T., Schwarz, T. L. and Tsien, R. W. (1993). Distinctive pharmacology and kinetics of cloned neuronal Ca^{2+} channels and their possible counterparts in mammalian CNS neurons. *Neuropharmac.* **32**, 1075–1088.